Received: 28 October 2016 | Revised: 13 December 2016 | Accepted: 7 January 2017

DOI 10.1002/jmor.20661

RESEARCH ARTICLE

WILEY

Post-metamorphic development of skin glands in a true toad: Parotoids versus dorsal skin

Eleonora Regueira[1,2*] | Camila Dávila[1*] | Alina G. Sassone[1] | María E. Ailín O'Donohoe[1,2] | Gladys N. Hermida[1]

[1]Facultad de Ciencias Exactas y Naturales, Departamento de Biodiversidad y Biología Experimental, Laboratorio de Biología de Anfibios-Histología Animal, Universidad de Buenos Aires, Buenos Aires, C1428EGA, Argentina

[2]Consejo Nacional de Investigaciones Científicas y Técnicas, Buenos Aires, C1033AAJ, Argentina

Correspondence
Gladys N. Hermida, Laboratorio de Biología de Anfibios-Histología Animal, Facultad de Ciencias Exactas y Naturales, Universidad de Buenos Aires, Intendente Güiraldes 2160, Ciudad Universitaria (C1428EGA), Buenos Aires, Argentina.
Email: gladyshermida@gmail.com

Funding information
Research support was provided by UBACyT 2014–2017 no. 20020130100828BA of the Universidad de Buenos Aires, República Argentina. Scholarship support for E.R. and M.E.A.O. was provided by the Consejo Nacional de Investigaciones Científicas y Técnicas, Argentina (CONICET).

Abstract

Chemical defenses in amphibians are a common antipredatory and antimicrobial strategy related to the presence of dermal glands that synthesize and store toxic or unpalatable substances. Glands are either distributed throughout the skin or aggregated in multiglandular structures, being the parotoids the most ubiquitous macrogland in toads of Bufonidae. Even though dermal glands begin to develop during late-larval stages, many species, including *Rhinella arenarum*, have immature glands by the end of metamorphosis, and their post-metamorphic growth is unknown. Herein, we compared the post-metamorphic development of parotoids and dorsal glands by histological and allometric studies in a size series of *R. arenarum*. Histological and histochemical studies to detect proteins, acidic glycoconjugates, and catecholamines, showed that both, parotoids and dorsal glands, acquire characteristics of adults in individuals larger than 50 mm; that is, a moment in which the cryptic coloration disappears. Parotoid height increased allometrically as a function of body size, whereas the size of small dorsal glands decreased with body size. The number of glands in the dorsum was not linearly related to body size, appearing to be an individual characteristic. Only adult specimens had intraepithelial granular glands in the duct of the largest glands of the parotoids. Since toxic secretions accumulate in the central glands of parotoids, allometric growth of parotoids may translate into greater protection from predators in the largest animals. Conversely, large glands in the dorsum, which produce a proteinaceous secretion of unknown function, grow isometrically to body size. Some characteristics, like intraepithelial glands in the ducts and basophilic glands in the dorsum, are limited to adults.

KEYWORDS
Bufonidae, chemical defense, granular glands, *Rhinella arenarum*

1 | INTRODUCTION

Amphibian skin is a complex organ with unique morphological, biochemical, and physiological characteristics among vertebrates (Clarke, 1997). The skin accomplishes diverse functions, for example, gas exchange, hydric and osmotic balance, excretion, thermoregulation, reproduction, and defense against predators and microorganisms (Brunetti et al., 2015; Clarke, 1997; Ferraro, Topa, & Hermida, 2013; Jared et al., 2005; Mailho-Fontana et al., 2014; Navas, Jared, & Antoniazzi, 2002; Toledo & Jared, 1993, 1995). In adults, the skin is formed by an epidermis with an underlying dermis that contains two morphological types of exocrine glands: acinar glands (commonly known as mucous glands), and syncytial glands which lumen is full of secretion (commonly known as serous, granular, or poison glands; Duellman & Trueb, 1994; Jared et al., 2009; Regueira, Dávila, & Hermida, 2016). Because the chemical nature of the accumulated secretion in syncytial glands varies (Clarke, 1997; Daly, 1995; Daly, Spande, & Garraffo, 2005; Rash Morales, Vink, & Alewood, 2011; Sciani, Angeli, Antoniazzi, Jared, & Pimenta, 2013) and because it has a granular appearance (Brunetti, Hermida, & Faivovich, 2012; Ferraro et al., 2013; Regueira et al., 2016), we prefer the term granular glands instead of syncytial glands.

*These authors contributed equally to this study.

The role of the skin as a chemical defense organ in anurans is related to the presence of unpalatable or toxic chemicals in the granular glands (Clarke, 1997; Daly, 1995; Toledo & Jared, 1995). True toads belonging to the Bufonidae produce highly toxic skin secretions, which are composed of cardiotonic steroids and biogenic amines like catecholamines, with a powerful vasopressor action in vertebrates (Cunha Filho et al., 2005; Maciel et al., 2003; Sciani et al., 2013; Toledo & Jared, 1995). Granular glands are distributed throughout the integument or arranged in "macroglands" (Antoniazzi, Neves, Mailho-Fontana, Rodrigues, & Jared, 2013; Brunetti et al., 2015; Jared et al., 2009, 2014; Lenzi-Mattos et al., 2005; Vences et al., 2007); the parotoid glands are the most ubiquitous macrogland in bufonids (Toledo & Jared, 1995). Parotoids are not only accumulations of granular glands but also specialized regions of the integument which contain different gland types, with a histological organization that confers functional features beyond a typical passive defense mechanism against predators (Almeida, Felsemburgh, Azevedo, & Brito-Gitirana, 2007; Jared et al., 2009; Mailho-Fontana et al., 2014; Regueira et al., 2016; Toledo, Jared, & Brunner, 1992).

Skin glands develop during the late larval stages (for review see Chammas, Carneiro, Ferro, Antoniazzi, & Jared, 2015; Regueira et al., 2016; Terreni, Nosi, Greven, & Delfino, 2003), and some species have different types of granular glands with changing characteristics throughout metamorphosis (Delfino, Brizzi, Alvarez, & Kracke-Berndorff, 1998; Delfino, Brizzi, Kracke-Berndorff, & Alvarez, 1998; Delfino, Brizzi, Alvarez, & Taddei, 1999; Regueira et al., 2016). During the post-metamorphic life, the skin of several *Rhinella* toads does not have the appearance of adults, which is evidenced both by its color pattern as by its histological structure (Chammas et al., 2015; Freeland & Kerin, 1991; Regueira et al., 2016). However, it is not clear if small juveniles have biologically active secretions. Freeland and Kerin (1991) observed in the field that individuals of *Rhinella marina* are toxic since metamorphosis, supporting the idea that all life stages of bufonids are toxic to predators. However, a chemical analysis showed that consumption of *R. marina* eggs killed tadpoles of two Australian frog species (*Limnodynastes convexiusculus* and *Litoria rothii*), whereas no tadpoles died after consuming late-stage *R. marina* tadpoles or small metamorphs (Hayes, Crossland, Hagman, Capon, & Shine, 2009). Furthermore, histological studies showed that during development of *Rhinella arenarum*, glands have small amounts of secretion with different histochemical properties than the skin of adults (Regueira et al., 2016). This background shows that it is not clear whether small juveniles have the same chemical skin defenses as adults.

Predator–prey interactions depend on body size and habits of individuals among other factors, and individuals in different stages of growth use different defense strategies (Hayes et al., 2009; Phillips & Shine, 2006). In toads belonging to the *R. marina* group (Maciel, Collevatti, Colli, & Schwartz, 2010), small juveniles are spit out unharmed by predators because of the presence of toxic or unpalatable substances in their skin (Freeland & Kerin, 1991); but larger animals eject their parotoid gland content when injured (Jared et al., 2009). These examples show that gland defense mechanisms are different throughout ontogeny; although, it is unknown how size, distribution, and capacity of synthesis of granular glands vary during development and in relation to changes in body size. A morphometric study of granular glands and body size in a dendrobatid poison frog showed that adults have a larger capacity to store alkaloids than juveniles, which may translate into greater protection from predators in adults (Saporito, Isola, Maccachero, Condon, & Donnelly, 2010). Further, a chemical study of alkaloids and bufotenin in the poison bufonid *Melanophryniscus moreirae*, discovered that the relationship between alkaloid richness and age appears to result from the gradual accumulation of alkaloids over a frog's lifetime, whereas the relationship between the quantity of defensive chemicals and size appears to be due to the greater storage capacity of larger individuals (Jeckel, Saporito, & Grant, 2015).

By the end of metamorphosis, skin glands in *R. arenarum* have immature morphological characteristics, and evidence of different types of granular glands is lacking (Regueira et al., 2016). With this background, the purpose of our study was to compare the post-metamorphic morphological changes in skin glands from the dorsum and parotoid, and to evaluate if the gland size and density changes in relation to body size in a size series of *R. arenarum*.

2 | MATERIALS AND METHODS

2.1 | Animals

Juvenile and adult specimens of *R. arenarum* (Hensel, 1867) were from the herpetological collection of Facultad de Ciencias Exactas y Naturales, Universidad de Buenos Aires (FCEN-DBBE) or recently collected and introduced to the herpetological collection of Facultad de Ciencias Exactas y Naturales, Laboratorio de Biología de Anfibios (FCEN-LBA). Young toadlets were obtained from collected tadpoles reared in dechlorinated tap water under natural photoperiod and temperature conditions of the spring season of Buenos Aires city in October 2014, and fed *ad libitum* with boiled chard. Metamorphosed individuals were reared under natural outdoor conditions of the spring season of Buenos Aires city for 10 days. Recently collected animals were euthanized by immersion in 1% aqueous solution of MS222 (tricaine methanesulfonate; Sigma-Aldrich, St. Louis, MI, USA) and fixed in 10% formaldehyde. Left parotoids were excised and fixed in Bouin's liquid to preserve the histological characteristics of the skin glands. Only two of the smallest individuals (snout-vent length = 11.26 and 11.8 mm) were completely fixed in Bouin's liquid because it was too difficult to separate the parotoid gland from the body without damaging it. Specimens from herpetological collection were fixed in 10% formaldehyde and stored in 70% ethanol. According to the absence/presence of macroscopically differentiated gonads individuals were categorized as adult male or female or as juvenile. Because in *R. arenarum* skin glands are not sexually dimorphic (Regueira et al., 2016), both sexes were used collectively to compare gland development with body size. Information regarding individuals employed for this study is summarized in Table 1.

This study was carried out according to the regulations specified by the Institutional Animal Care and Use Committee of the Facultad de Ciencias Exactas y Naturales, UBA (Res C/D 140/00). The

TABLE 1 Information regarding specimens employed for the present study

Life stage	SVL (mm)	Number of specimens	Source	N° of specimen	Location/date of collection
Young toadlets	11.26-13.96	4	Ciudad Universitaria, Buenos Aires City, Argentina	FCEN-LBA n° 126, 127, 128, 129	34°32′S, 58°27′W/October 2014
Juveniles	15.36-67.00	5	La Reja, Buenos Aires Province, Argentina	FCEN-LBA n° 121, 122, 123, 124, 130	34°38S, 58°48W/January-March 2014
Juveniles	24.85-51.19	4	Herpetological collection of FCEN-DBBE	FCEN-DBBE n° 10 spec. 2, 3	34°38′S, 58°28′W/October 1960
				FCEN-DBBE n° 907 spec. 2	34°45′S, 58°14′W/May 1962
				FCEN-DBBE n° 1217 spec. 1	31°10′S, 64°19′W/February 1963
Adults	77.53-101.10	6 (4 ♂ and 2 ♀)	Herpetological collection of FCEN-DBBE	FCEN-DBBE n° 15, spec. 6	34°36′S, 58°38′W/October 1960
				FCEN-DBBE n° 641, spec. 4, 5, 9, 11	29°48′S, 64°43′W/October 1961
				FCEN-DBBE n° 1928, spec. 3	36°30′S, 61°34′W/November 1967

SVL=snout-vent length; spec.=specimen.

Conservation category of *R. arenarum* is "Least concerned" according to the IUCN Red List criteria (IUCN, 2016) and Vaira et al. (2012).

2.2 | Samples and histological preparations

Histological changes in skin glands and morphometric relationship between parotoid glands, dermal glands in the dorsum and body size were investigated in the 19 specimens listed in Table 1. To cover the diversity of body sizes, we worked with animals with a snout-vent length (SVL) ranging from 10 to 100 mm, divided into ranges of 10 mm in length, being careful to have at least one individual in each size range. For histological analysis, samples of dorsal and ventral skin, as well as parotoid glands were embedded in paraplast (Sigma-Aldrich, St. Louis, MI), and then sectioned in a transverse plane at 6 μm thickness. Sections were stained with haematoxylin and eosin (H-E) for general cytology and histology, and the following histochemical stains were performed on selected sections to evaluate developmental changes in skin glands secretions: periodic acid-Schiff-haematoxylin (PAS-H; Kiernan, 1999) for neutral glycoconjugates, Alcian blue 8GX at pH 2.5 plus haematoxylin (AB-H; Kiernan, 1999) for primarily carboxylated acidic glycosaminoglycans, and Coomassie blue R250 (Coom; Kiernan, 1999) for proteins. Mucous glands of adult skin and cartilage of tadpoles were used as positive controls for PAS and AB; a keratinized portion of the dorsal epidermis of adults was used as a positive control for Coom. To detect catecholamines in gland secretions, the chromaffin reaction (Chromaffin R-H) was applied to skin samples from recently collected specimens (Kiernan, 1999; Regueira et al., 2016).

To quantify the number and size of granular glands, a patch of skin from the same position of the dorsum of each toad was excised, which included the area of dorsal skin between the sixth and eighth vertebrae, inclusively, and 1/3 of the width of the animal between the spine and the lateral edge to both sides of the animal (Figure 1a). The length of the skin patch was calculated as the average length of a vertebra (*D*1) multiplied by 3, and *D*1 was estimated as the distance between the skull base and the sacrum, divided by eight, the total number of vertebrae (Figure 1a). The patch was excised from the anterior edge of the sacrum to the sixth vertebra (Figure 1a). Skin patches were individually embedded in paraplast, and serially cross-sectioned transversely at 10 μm section thickness. Sections were stained with H-E to differentiate basophilic and acidophilic glands in the dorsum (Regueira et al., 2016). Skin patch sizes were measured with dial calipers (.02 mm) and are given in millimeters.

All stained sections were examined using a Zeiss Primo Star microscope, and images were captured using a Canon PowerShot A640 digital camera. Low magnification pictures of the specimens were captured with a Nikon coolpix 995 3.34 Mp digital camera. The width of each section was measured with AxioVision software (Zeiss).

2.3 | Parotoid gland morphological measurements

To study the relationship between body size and growth of parotoid glands, the area and height of one macrogland was measured for each specimen. Previous to this study, we compared the external morphology and number of glands, in left and right parotoids of one individual. The comparison showed that both parotoid glands have a similar morphology and histological organization, and are composed of a similar number of central and peripheral glands (data not shown). For this reason, we randomly chose to compare right parotoid glands. Area was approached as the sum of an upper oval plus the area of a triangle below (Figure 1b). The area of the oval was calculated as $\pi.r1.r2$ (where $r1$ = the longest straight line between the anterior and posterior portion of the oval divided by 2 and $r2$ = oval width measured at half the

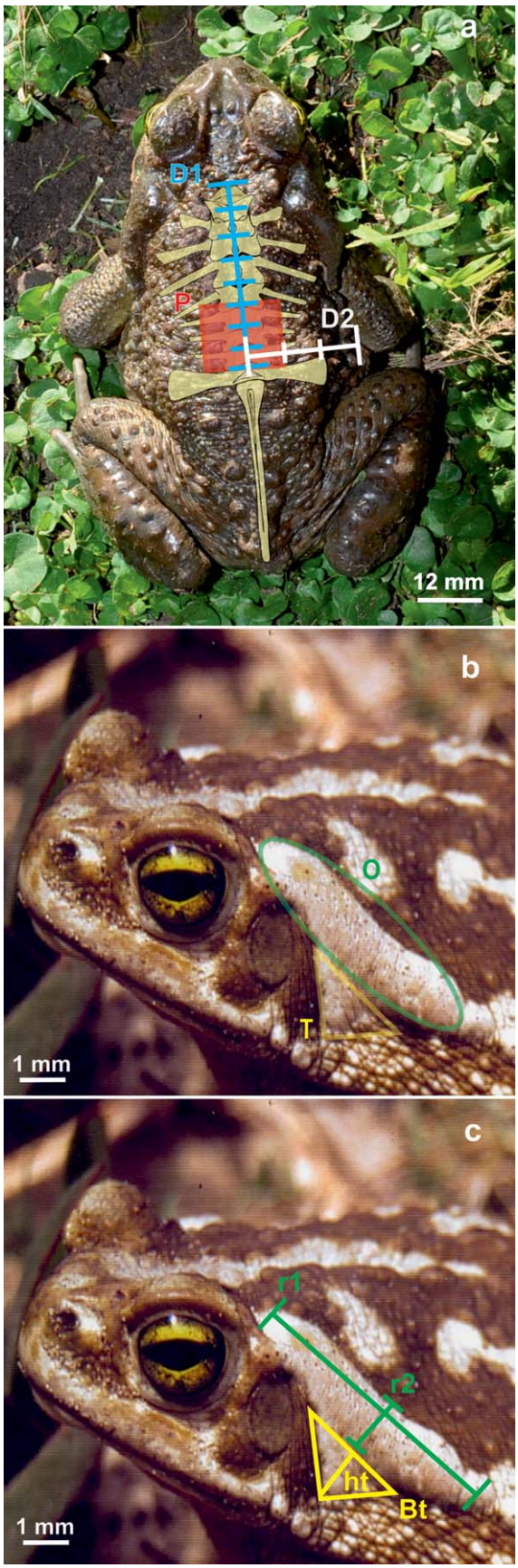

FIGURE 1.

base of the lower triangle divided by 2; Figure 1c). The area of the isosceles triangle that approximates the lower portion of parotoid gland was estimated as Bt.ht/2 (where Bt = the base of the triangle and ht = height of the triangle; Figure 1b). The maximum height of parotoid glands was estimated by measuring the maximum height of the macrogland in several transverse histological sections of the highest portion of the macrogland. We used Axiovision software (Zeiss) to measure the length between the deepest border of the largest central gland to the top of epidermis, avoiding the problem of losing different amounts of *stratum compactum* below the glands during histological preparation. Those animals whose parotoid glands were not externally observed (SVL < 13.96 mm) and animals without the triangle portion of parotoid glands (SVL < 33.09 mm) were not included in the statistical analysis of parotoid gland area development.

2.4 | Dorsal skin glands morphological measurements

Because we found that the skin of *R. arenarum* is heterogeneous regarding size of the granular glands in the dermis, we decided to take two reference measurements to compare animals of different sizes: the average diameter of small granular glands and diameter of the largest granular gland. The former was evaluated from measurements of 15 randomly selected small granular glands from each skin patch, and was calculated by following individual glands through serially adjacent skin sections, summing the number of sections each gland spanned, and multiplying this number by the section thickness of 10 μm. The diameter of the largest gland was estimated in a similar manner, by following serial sections of the first large gland observed in the skin patch. Based on the work of Saporito et al. (2010), this value was employed to determine the *sampling strata* to count the number of skin glands without counting any gland more than once. After sectioning the whole skin patch, and dividing sections into *sampling strata*, we measured the diameter of other large glands, and ascertained that large glands of one individual have similar diameter.

The total number of glands in the skin was estimated in the selected dorsal skin patch, and was calculated following a modified protocol by Saporito et al. (2010). Modifications in the protocol relate to the fact that *R. arenarum* has large and small granular glands, and *Oophaga pumilio* has only one type of skin gland. To minimize over counting glands that appeared in more than one skin section, serial sections from each toad were divided into *sampling strata* equal to

FIGURE 1 *R. arenarum*, morphometric parameters measured in specimens of the size series. (a) Graphic representation of the skin patch (red rectangle) employed to study the size, number, and density of skin glands. *D*1 indicates the average length of a vertebra. *D*2 is 1/3 of the width of the animal between the spine and the lateral edge of the animal. Image by Raúl Orencio Gómez. (b) Parotoid gland outlined as an oval (O, green) and a triangle (T, yellow). (c) Parameters shows employed to measure the area of the oval and triangle that forms the parotoid. *r*1 = the longest straight line between the anterior and posterior portion of the oval; *r*2 = oval width measured at half the base of the lower triangle. Bt = the base of the triangle; ht = height of the triangle. (b) and (c) image by Ariel López

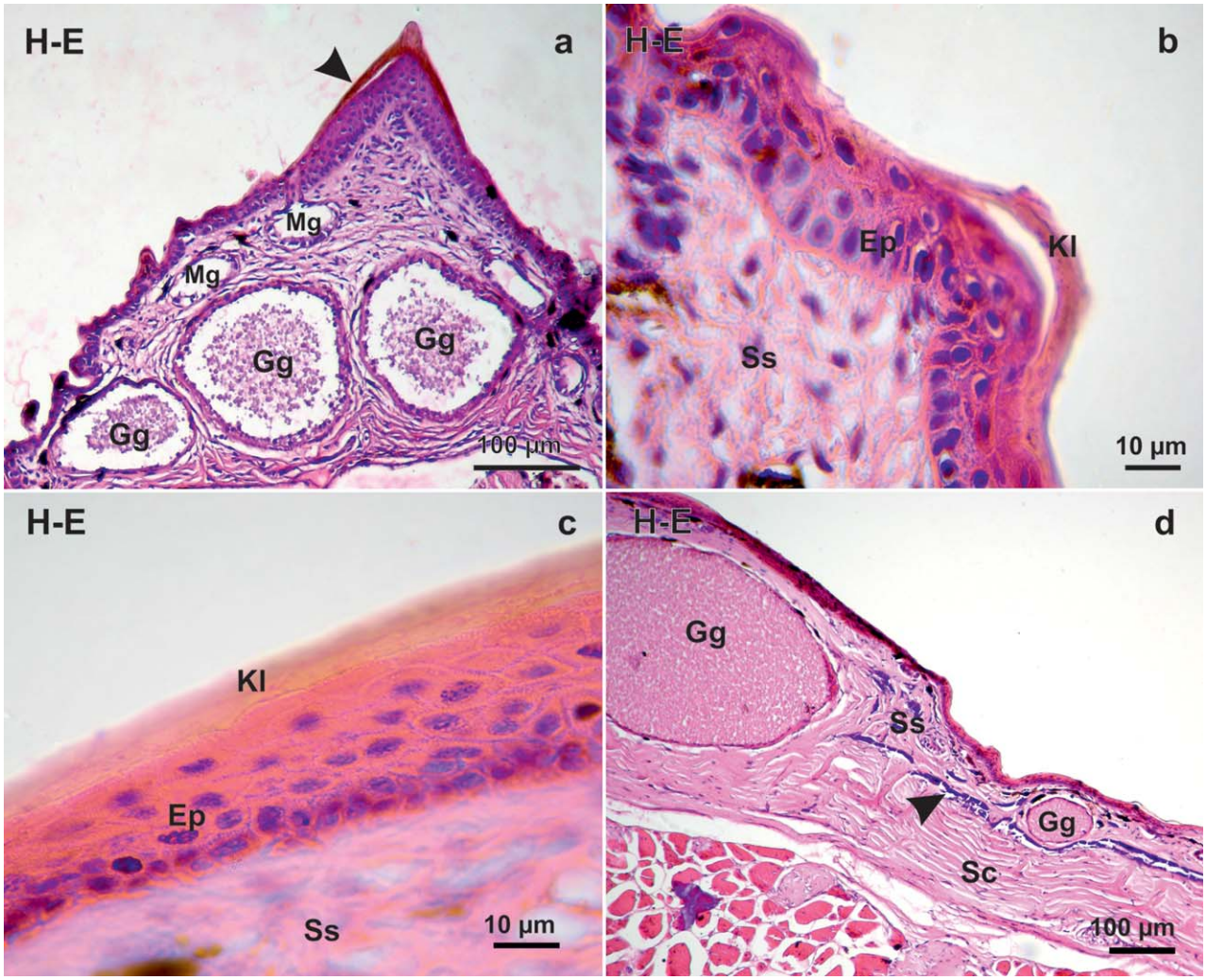

FIGURE 2 *R. arenarum*, dorsal skin during juvenile growth. H-E staining. (a) Wart in a juvenile of 33.09 mm. Notice the cornified epidermal spine (arrowhead) on the top of the wart, and the presence of mucous and granular glands in the *stratum spongiosum* of the dermis. (b) Detail of epidermis in a juvenile of 33.09 mm. Observe the presence of a desquamated *stratum corneum*. (c) Detail of epidermis in a juvenile of 62.5 mm. Notice that epidermis had a higher degree of keratinization of the *stratum corneum*. (d) Skin in juvenile of 67 mm. The dermis had large and small granular glands, and the basophilic Eberth–Kastschenko layer (arrowhead) was already developed between the *stratum spongiosum* and *stratum compactum*. Epidermis (Ep); Granular gland (Gg); Keratin layer (Kl); Mucous gland (Mg); S*tratum compactum* (Sc); *Stratum spongiosum* (Ss)

diameter of the first large gland observed in the skin patch. *Sampling strata* were calculated by dividing the total number of sections obtained from a patch of an individual by the diameter of the first large gland observed for that same individual. Granular glands were counted per *stratum* by viewing one section from edge to edge and recording all glands observed. Plots of gland frequency (n° of glands/mm) for different *strata* from different individuals established that poison glands are evenly distributed across skin sections (data not shown). Because each *stratum* was defined by the diameter of large glands, the quantification of small glands is underestimating the total number of small glands; for this reason we used the following equation, to estimate the total number of granular glands present in the skin patch:

$$\hat{n}^{\circ}\text{ of glands in skin patch} = n^{\circ}\text{ of large glands} + \hat{n}^{\circ}\text{ of small glands} \quad (1)$$

where $\hat{n}^{\circ}$ is the estimated number of whichever applies.

In Equation 1, the estimated number of small glands was calculated as:

$$\hat{n}^{\circ}\text{ of small glands} = \frac{\text{skin patch length}}{\hat{\varnothing}\text{ of small glands}} \times \frac{(\text{total } n^{\circ}\text{ of counted glands} - n^{\circ}\text{ of large glands})}{\text{stratum length}} \quad (2)$$

where $\hat{\varnothing}$ is the estimated diameter of glands.

The estimated number of granular glands per skin patch was used to calculate the gland density, as follows:

$$\text{Granular gland density} = \frac{\hat{n}^{\circ}\text{ of glands in skin patch}}{\text{skin patch area (in mm}^2\text{)}} \quad (3)$$

2.5 | Null model of parotoid gland growth and statistical analysis

To examine the growth of parotoid glands in *R. arenarum* as a function of overall growth in toad size (SVL), we studied the isometric/allometric

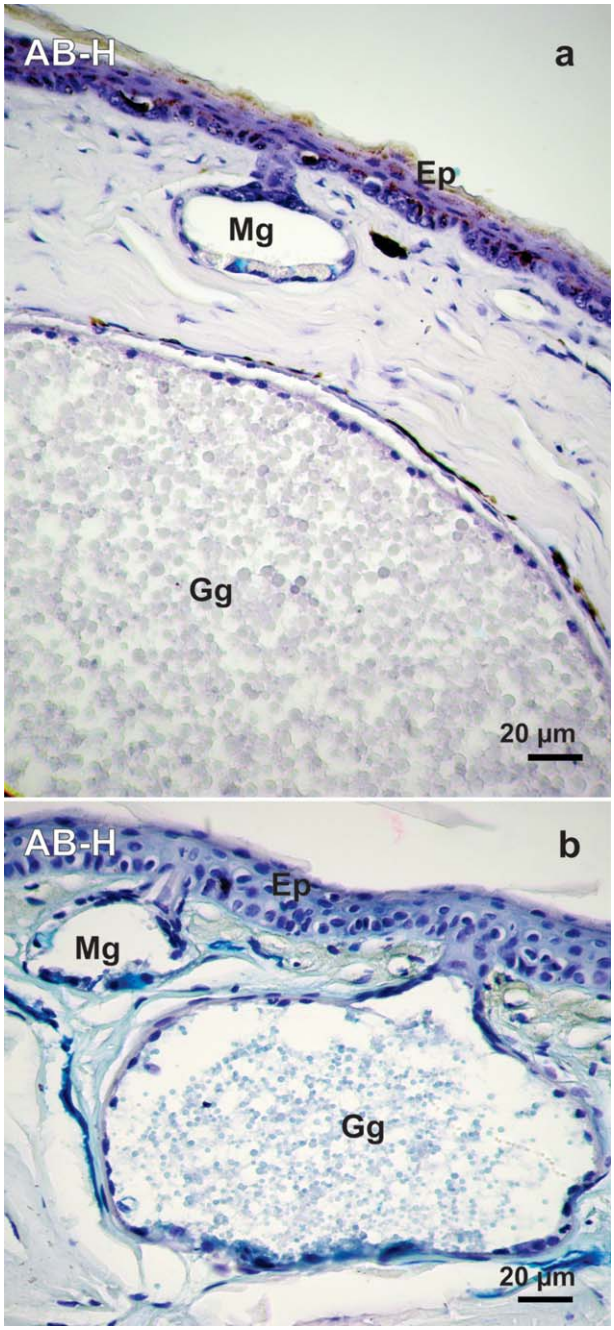

FIGURE 3 *R. arenarum*, acidic glycoconjugates in (a) dorsal and (b) ventral skin glands of toads with SVL = 50.68 mm. AB-H staining. (a) Some cells in mucous gland acinus were positive for AB and the content inside granular gland was negative for AB. (b) Notice that ventral mucous gland were similar to dorsal skin. Differently, ventral granular glands had a granular content slightly positive for AB. Epidermis (Ep); Granular gland (Gg); Mucous gland (Mg)

relationship between both variables. Isometric scaling is the simplest scaling relationship, in which changes in one parameter are accompanied by equivalent changes in another, and can serve as a null hypothesis against which observed changes in growth can be compared (Saporito et al., 2010; Schmidt-Nielsen, 1984). The scaling relationship between parotoid gland size (length, area, and height) and body growth was examined using reduced major axis (RMA) linear regression analysis, which accounts for error in both the dependent and independent variables (Warton, Wright, Falster, & Westoby, 2006).

Assumptions of RMA linear regression, that is, normal distribution, homocedasticity, and independence of residuals, were tested with PAST Software (version 2.17c; Hammer, Harper, & Ryan, 2011). Log10-transformed size variables were considered to be linearly related with a correlation coefficient $R^2 > 0.8$. Slopes values and 95% confidence intervals of the RMA linear slopes for each regression were calculated with PAST Software. To determine if the scaling relationships were isometric or allometric, values were compared to a null hypothesis of an isometric slope equal 1 or 2, depending on the dimensional exponent of the variables. When comparing variables expressed in the same dimension (e.g., parotoid gland height in mm vs. body size in mm), the exponent of a hypothetic isometric relationship equals 1, and then the slope of the linear function that better describes that relationship is expected to be 1. However, when the independent variable is expressed in one dimension and the dependent variable is in two dimensions (e.g., parotoid gland area in mm^2 vs. body size in mm), the exponent of a hypothetic isometric relationship equals 2 and the slope is expected to be 2. A scaling relationship was statistically considered allometric if the 95% confidence interval for its slope did not contain the expected slope for isometry (Saporito et al., 2010).

3 | RESULTS

3.1 | Morphological changes in skin glands during post-metamorphic growth

The skin of juveniles with SVL = 33.09 mm already had warts and spines, similarly to adults (Figure 2a). At this stage of development, the epidermis was already keratinized; although, the corneous layer was thinner than in adults and the number of epidermal layers was four (Figure 2b). From 50.68 mm long, the skin had the appearance of adults regarding the following features: number of epidermal layers (5–6 layers; Figure 2c), presence of a basophilic dermal layer between the *stratum spongiosum* and *stratum compactum* (also known as the Eberth–Kastschenko layer; Azevedo et al., 2005; Figure 2d), and morphology and histochemical characteristics of dorsal (Figures 2d and 3a) and ventral glands (Figure 3b). From SVL = 50.68 mm onwards, the dorsum had large and small granular glands with acidophilic granules (Figure 2d), and mucous glands had some cells with acidic glycoconjugates (Figure 3a). The ventral skin had granular glands with its content slightly positive for acidic glycoconjugates (Figure 3b), and mucous glands had the same characteristics as those of the dorsal skin (Figure 3b). Interestingly, in juveniles, none of the large granular glands in the dorsum had a basophilic content, as it occurs in the largest Type B glands of adults (see Regueira et al., 2016; for further detail regarding these glands).

In adults, the parotoid gland has an oval appearance in an anteroposterior position, and a triangular portion that protrudes from the middle region of the oval toward the ventral side (Figure 1b). Histologically,

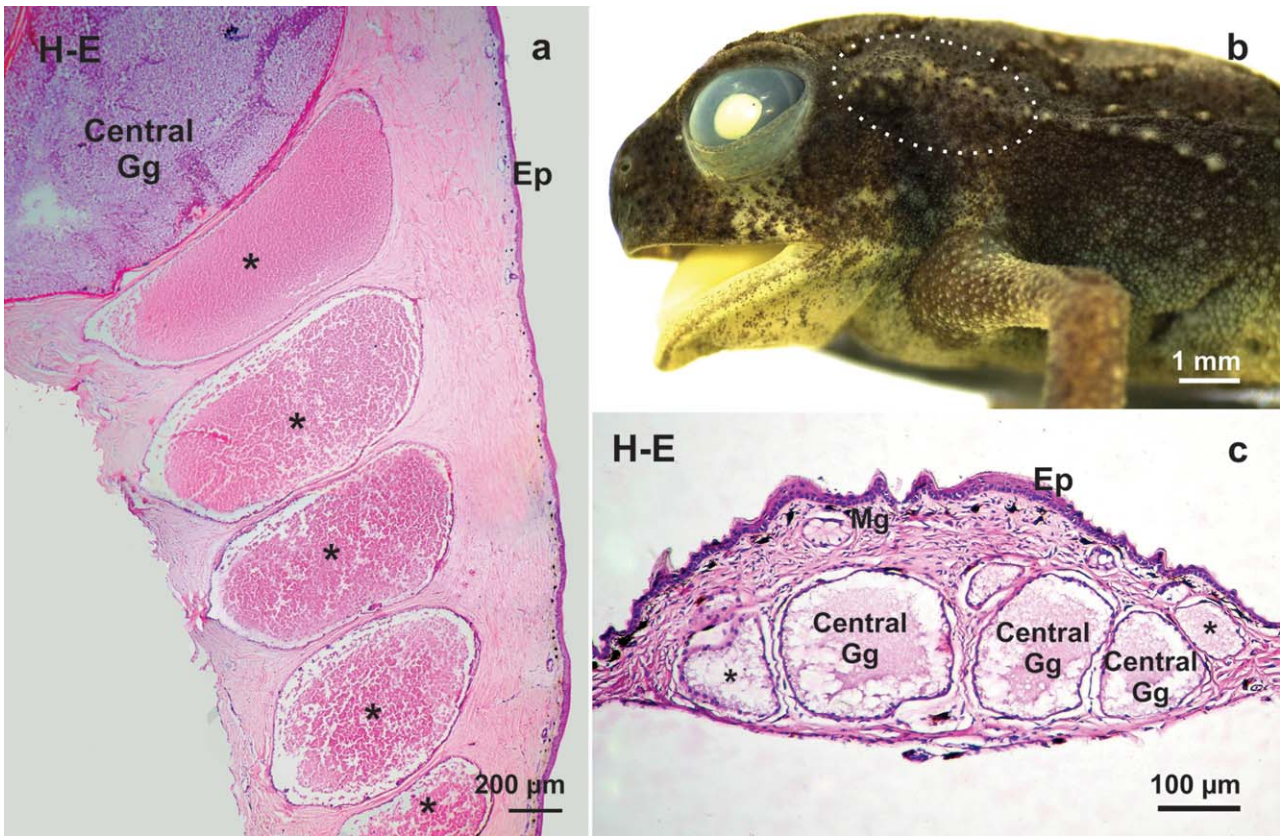

FIGURE 4 *R. arenarum*, parotoid gland development. (a) Lower region of parotoid gland in adult, showing the presence of large peripheral (acidophilic) glands. H-E staining. (b) Lateral view of juvenile with SVL of 11.90 mm fixed in Bouin's fluid. Observe that parotoid gland (white arrow) is less prominent than in adults. (c) Parotoid gland in juvenile of 15.36 mm. Notice that peripheral and central glands were not differentiable and gland content inside large granular glands was scarce. H-E staining. Central granular gland (Central Gg); Epidermis (Ep); Mucous gland (Mg); Peripheral gland (*)

the upper portion with oval shape, consisted of central (basophilic) and peripheral (acidophilic) glands and the lower triangular portion was a continuation of the peripheral glands toward the ventral side of the parotoid (Figure 4a). In juveniles shorter than SVL = 33.09 mm, parotoids were less evident than in it was possible adults (Figure 4b), and large granular glands had an immature appearance with scarce and

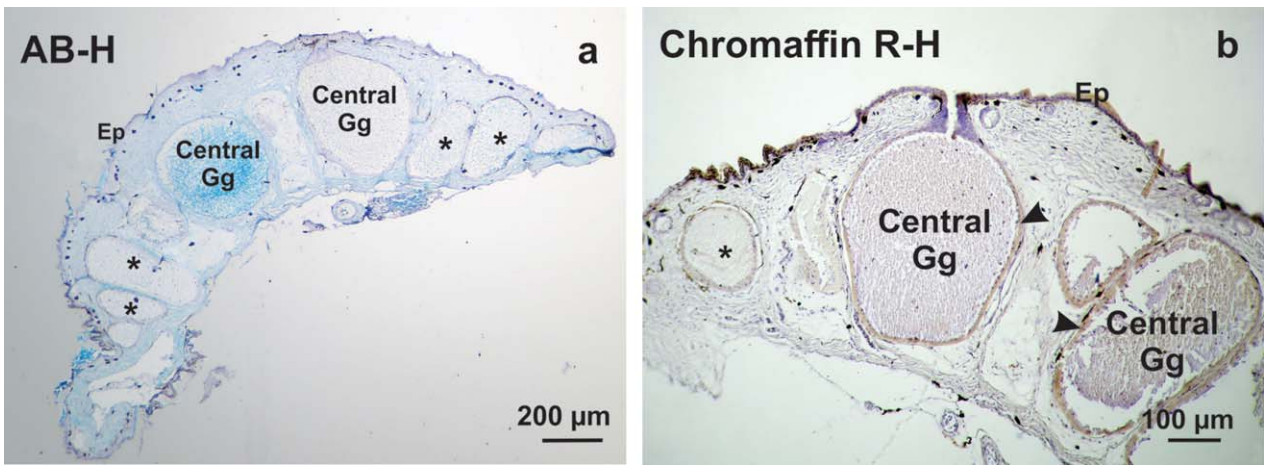

FIGURE 5 *R. arenarum*, transverse section of parotoid gland in a juvenile with SVL = 33.09 mm. Peripheral and central glands could be distinguished in animals larger than this size. (a) Central glands were larger than peripheral glands, and some of the central glands were positive for detection of acidic glycoconjugates. AB-H staining. (b) The perinuclear cytoplasm of the syncytium in the central glands was positive (brownish color; arrowhead) for catecholamines. Chromaffin R-H staining. Central granular gland (Central Gg); Epidermis (Ep); Peripheral gland (*)

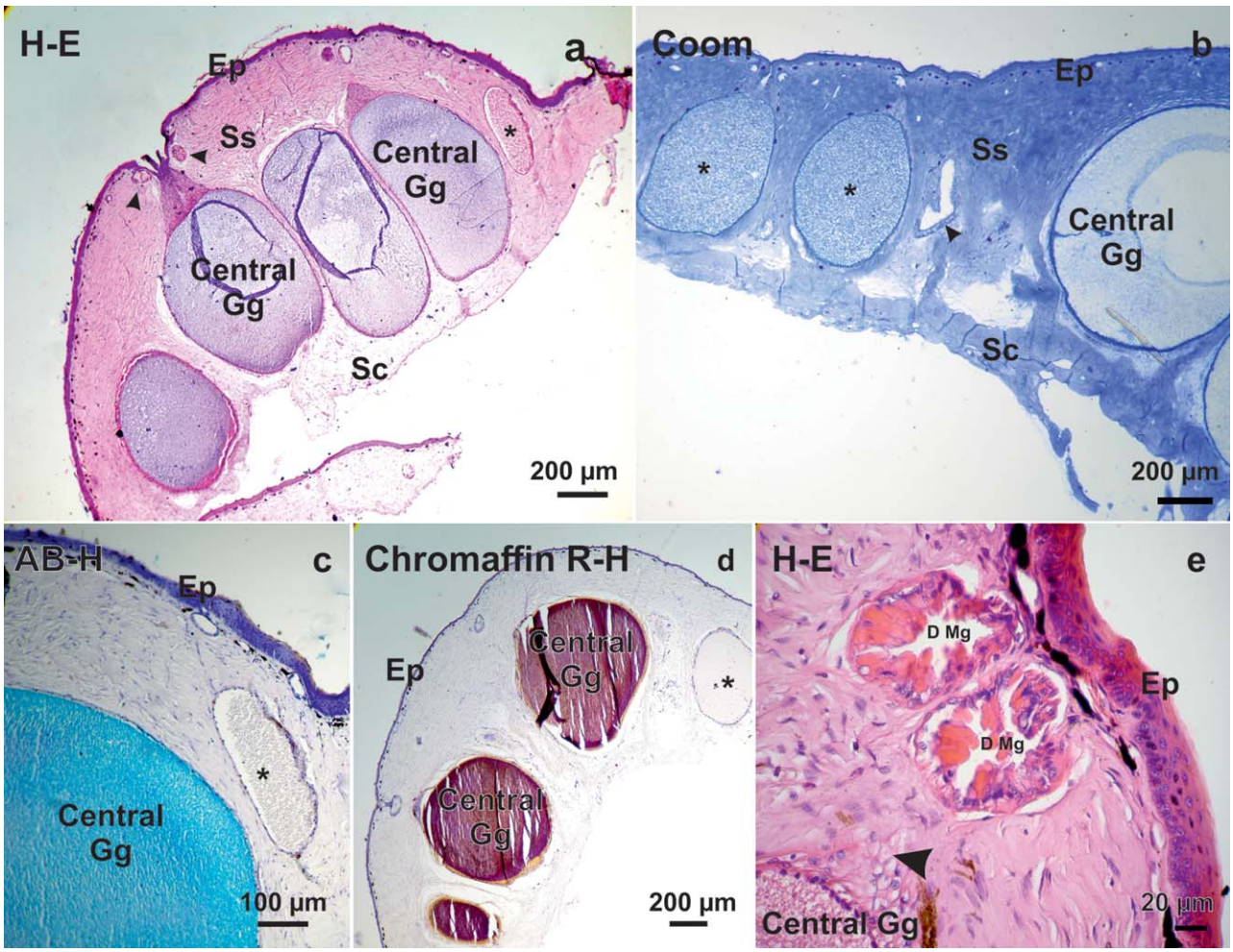

FIGURE 6 *R. arenarum*, parotoid gland of a juvenile with SVL = 50.68 mm. The macrogland had the same histological organization and histochemical properties of adults. (a) Observe the large and crowded central glands in the oval region of parotoid, with abundant basophilic secretion. Arrowheads point to differentiated mucous glands around the neck of central gland. H-E staining. (b) Peripheral glands in the triangular portion of parotoid were slightly positive for protein detection but central glands were negative, similarly to adults. Observe a discharged gland (arrowhead) between the central and peripheral glands in the oval and triangular region of parotoid, respectively. Coom staining. (c) Central glands had abundant content, positive for acidic glycoconjugates. AB-H staining. (d) Content inside central glands was positive for catecholamine detection. Chromaffin R-H staining. (e) Detail of differentiated mucous glands around the neck of central glands. Arrowhead points to central gland neck. H-E staining. Observe position of differentiated mucous glands in (a). Central granular gland (Central Gg); Differentiated mucous gland (D Mg); Epidermis (Ep); Peripheral gland (Peripheral Gg); *Stratum compactum* (Sc); *Stratum spongiosum* (Ss)

shrinked content (Figure 4c). Central and peripheral glands had the same histological characteristics and could not be distinguished from each other, as in adults (Figure 4a,c). The adult external morphology of the parotoid was documented in juveniles with SVL larger than 33.09 mm, which coincides with the stage in which central and peripheral glands can be histologically differentiated by the presence of acidic glycoconjugates in some of the central glands (Figure 5a), and by the detection of catecholamines in the perinuclear cytoplasm of syncytia in central glands (Figure 5b). Juveniles with SVL larger than 50.68 mm had parotoid glands with the same histological organization and histochemical properties of adults: enlarged and crowded peripheral and central glands (Figure 6a), with peripheral glands positive for protein content (Figure 6b), and central glands positive for acidic glycoconjugates and catecholamines (Figure 6c,d). In juveniles with SVL larger than 50.68 mm, differentiated mucous glands, with acidophilic columnar cells, surrounded the neck of central glands (Figure 6e).

Only in adults, the duct of central and peripheral glands of parotoids have intraepithelial granular glands (Figure 7a) with a content positive for acidic glycoconjugates (Figure 7b,c).

3.2 | Morphometric changes in parotoid glands during post-metamorphic growth

The external morphology of the parotoid gland changes during juvenile growth due to the development of large granular glands in the most ventral portion of the parotoid (Figures 1b and 4a). For this reason, the estimation of the total area of parotoid changed through ontogeny, being considered as an oval in juveniles smaller than 33.09 mm, and as

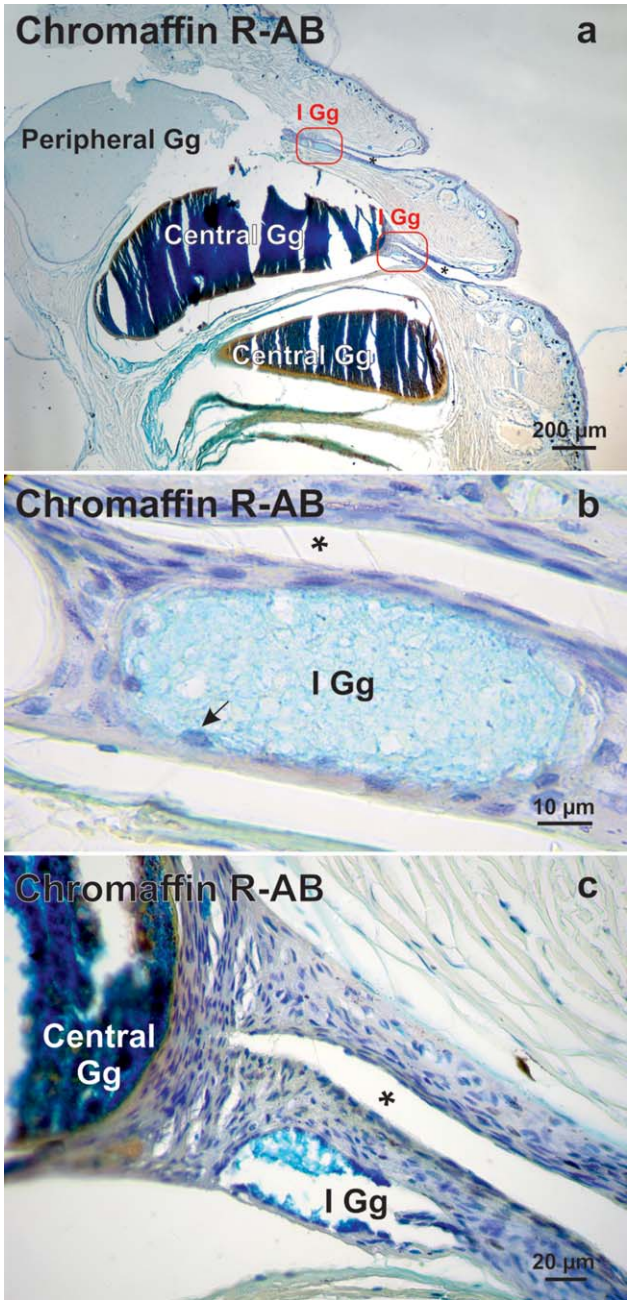

FIGURE 7 *R. arenarum*, intraepithelial granular glands in the duct of central and peripheral glands of parotoids of adult individuals. (a) Low magnification photograph of parotoid showing the position of intraepithelial granular glands (red squares) in peripheral and central glands. Chromaffin-AB staining. (b) Detail of the duct of peripheral gland shown in (a) Arrow indicates nucleous of syncytium of the gland. Notice the granular content, positive for acidic glycoconjugates. (c) Detail of the duct of central glands shown in (a), showing that intraepithelial glands have the same morphology as in duct of peripheral glands. Central granular gland (Central Gg); Intraepithelial granular gland (I Gg); Lumen of the gland duct (*); Peripheral gland (*)

the sum of an upper oval plus a lower triangle, in animals larger than 33.09 mm. The slope of the RMA regression line for the total area of parotoid gland was 2.19 (Figure 8a; 95% CI = 1.98–2.49; $R^2 = 0.97$), suggesting an isometric relationship between total area of parotoid and SVL. Although the area of parotoid is a good parameter to evaluate the intraspecies growth of the macrogland, it is not appropriate for interspecies comparison because parotoid glands have a dissimilar shape in different species of anurans. For this reason, data related to the length of the macrogland is also presented. Length of parotoids (*r*1 in Figure 1) increased from 2 mm in the smallest toadlet to a maximum of 25 mm in an adult, and the slope of the RMA regression line was 1.05 (Figure 8b; 95% CI = 0.99–1.15; $R^2 = 0.98$), suggesting an isometric relationship between length of parotoid and SVL.

The height of the parotoids increased with body size (Figure 8c), from .08 mm in the smallest toadlet to 2.68 mm in adults. The slope of the RMA regression line for the height of parotoid gland was 1.45 (95% CI = 1.35–1.60; $R^2 = 0.97$), suggesting a positive allometric relationship between height of parotoid and SVL.

3.3 | Morphometric changes in dorsal skin glands during post-metamorphic growth

Both average diameter of small glands and diameter of the largest granular gland, increased with increasing body size (Figure 9a,b), but at a different rate. Largest gland diameter increased from 98 µm at 11.26 mm SVL to 1116 µm at 101.1 mm SVL and the slope of the RMA regression line was estimated as 1.05 (Figure 9a; 95% CI = 0.92–1.19; $R^2 = 0.88$), suggesting an isometric relationship between size of larger glands and SVL. Small gland diameter increased from a mean of 91.63 µm at 11.26 mm SVL to 431.4 µm at 101.1 mm SVL and the slope of the RMA regression line was 0.64 (Figure 9b; 95% CI = 0.52–0.77; $R^2 = 0.83$), indicating a negative allometric relationship between small gland size and SVL.

The estimated number of glands per skin patch as dependent variable of SVL (Figure 9c). Was supported by a low RMA linear regression coefficient of determination ($R^2 = 0.45$), which was below the criteria established as good fitness to a linear relationship ($R^2 > 0.8$). For this reason, the allometric relationship between number of glands per skin patch and SVL was not be studied. Finally, granular gland density (n° of granular glands/mm^2) decreased with increasing body size (Figure 9d). The slope of the RMA regression line was calculated as −1.97 (95% CI = −2.35 to −1.74; $R^2 = 0.89$), suggesting a negative relationship between granular gland density and SVL.

4 | DISCUSSION

The glands of the integumentary system of *R. arenarum* are immature in young post-metamorphs. Therefore, post-metamorphic development is crucial for the functional differentiation of the skin defense system. Dorsal glands and parotoid macroglands acquire the morphological and histochemical characteristics of adults at the same body size (around 50 mm long), which according to Echeverría and Filipello (1990) is before they reach sexual maturity. Up to snout-vent length (SVL) = 50 mm, granular glands have an immature appearance, with scarce content and heterogeneous granules, similar to gland morphology in

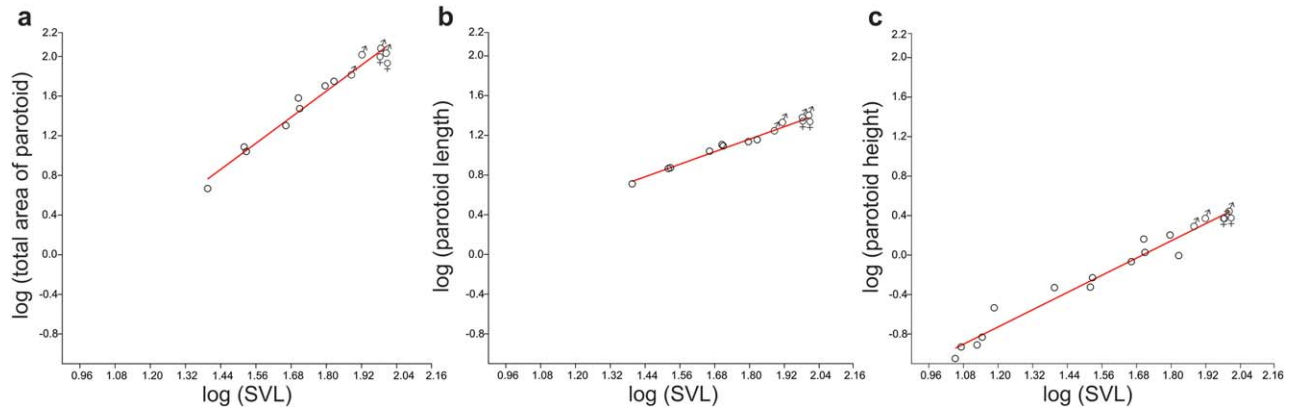

FIGURE 8 *R. arenarum*, relationship between parotoid gland morphometric parameters and body length (a) total area, (b) length, and (c) height of parotoids. Red lines in graphs represent the RMA regression estimated line. Juveniles are indicated by circles, and males and females are indicated by their respective symbols. Area and length were only measured in specimens where parotoid glands were evident to the naked eye ($n = 14$). Height was measured in histological sections of all specimens ($n = 19$)

tadpoles of several anuran species (summarized by Terreni et al., 2003); however, we cannot rule out that the content is secreted and/or accomplishes a biological function. Comparing with other bufonids, *Rhinella marina* is apparently toxic from metamorphosis (Freeland & Kerin, 1991), and the parotoid glands of all *R. marina* irrespective of SVL, contain secretory products (Freeland & Kerin, 1991). Because *R. arenarum* and *R. marina* are closely related species (Maciel et al., 2010; Portik & Papenfuss, 2015), we suspect that although skin glands in juveniles of *R. arenarum* have an immature morphology, they have a biologically active secretion. To our knowledge, this is the first record of immature skin glands in large juveniles, and appearance of the adult gland morphology is coincident with disappearance of the cryptic coloration pattern (Regueira et al., 2016), which implies that defensive strategies changes once skin glands are fully matured.

In agreement with the previous hypothesis regarding the preponderance of parotoid glands in the skin defense system of bufonids (Almeida et al., 2007; Jared et al., 2009; Mailho-Fontana et al., 2014), this study shows that parotoids in *R. arenarum* grow at a faster rate than dorsal glands, becoming a functional macrogland with toxic components (Regueira et al., 2016). The allometric growth in height of parotoids is mainly due to growth of the large granular glands that almost fill the entire dermis. This implies that as toad growth progresses, parotoids accumulate increasing amounts of secretion. On the contrary, dorsal glands either grow isometrically, if they are the large glands, or at a lower rate than body size, if they are the small glands. An ontogenetic increase in parotoid gland size has also been reported for *R. marina*, an anuran capable of synthesizing defensive bufadienolides (Phillips & Shine, 2006), and rapid increase in the relative size of the parotoid glands begin once an SVL of 70 mm has been reached (Freeland & Kerin, 1991). With this background, we think that an exhaustive comparison between growth of dorsal glands and parotoids in diverse species of bufonids with different types of secretion and without parotoids would provide data to relate the diverse changes that occur in anuran skin with ontogenetic variations in other defense mechanisms. When comparing with non-bufonid species, during post-metamorphic growth of *Oophaga pumilio*, a dendrobatid frog which possesses granular glands that store and secrete alkaloid-based toxic chemicals (see Daly et al., 2005 for review), the size, number, and percentage of dorsal skin occupied by poison glands increase allometrically as a function of body size (Saporito et al., 2010), resulting in adults with a larger capacity to store alkaloids. As dendrobatids lack macroglands, increase in capacity to accumulate defensive secretions along ontogeny relies on dorsal glands, and similarly to parotoid scaling in *R. arenarum*, adults have a larger capacity to accumulate secretions. Adults of *R. arenarum* have in their parotoids and in the biggest warts of the dorsum, two types of granular glands: Type A, acidophilic, with proteinaceous content, and Type B, basophilic, with catecholamines, acidic glycoconjugates, and lipid-derived products (Regueira et al., 2016). Although the biological function of the secretion in each type of gland is unknown, Type B glands are presumably related with the defensive system because of the presence of catecholamines (Toledo & Jared, 1995). Catecholamine possessing glands are predominantly in the parotoids, thus, the allometric growth of parotoids in *R. arenarum* directly indicates an increase in the defensive chemical system through ontogeny.

One interesting result of our study is that estimated number of granular glands in the skin patch of dorsal skin is not linearly related with size of individuals. In contrast, the number of skin glands seems to be a trait characteristic of each individual toad, and intraspecific variation should be considered. To our knowledge, skin gland primordia (*anlagen*) are only present in the epidermis of tadpoles (Terreni et al., 2003 and papers cited therein; Chammas et al., 2015; Quinzio & Fabrezi, 2012; Regueira et al., 2016) and have not been described in the skin of adults or juveniles (Antoniazzi et al., 2013; Chammas et al., 2015; Jared et al., 2009; Regueira et al., 2016; Saporito et al., 2010). If this is the case, the number of skin glands in each individual would depend on the number of gland *anlagen* that develop during the larval life, and would be constant throughout the post-metamorphic life. Contradicting this hypothesis, and different from *R. arenarum*, Saporito et al. (2010) described that in *Oophaga pumilio*, the number of poison glands increases with SVL, but, because density decreases, they conclude that gland hyperplasia is minimal. Similar to gland density fall in

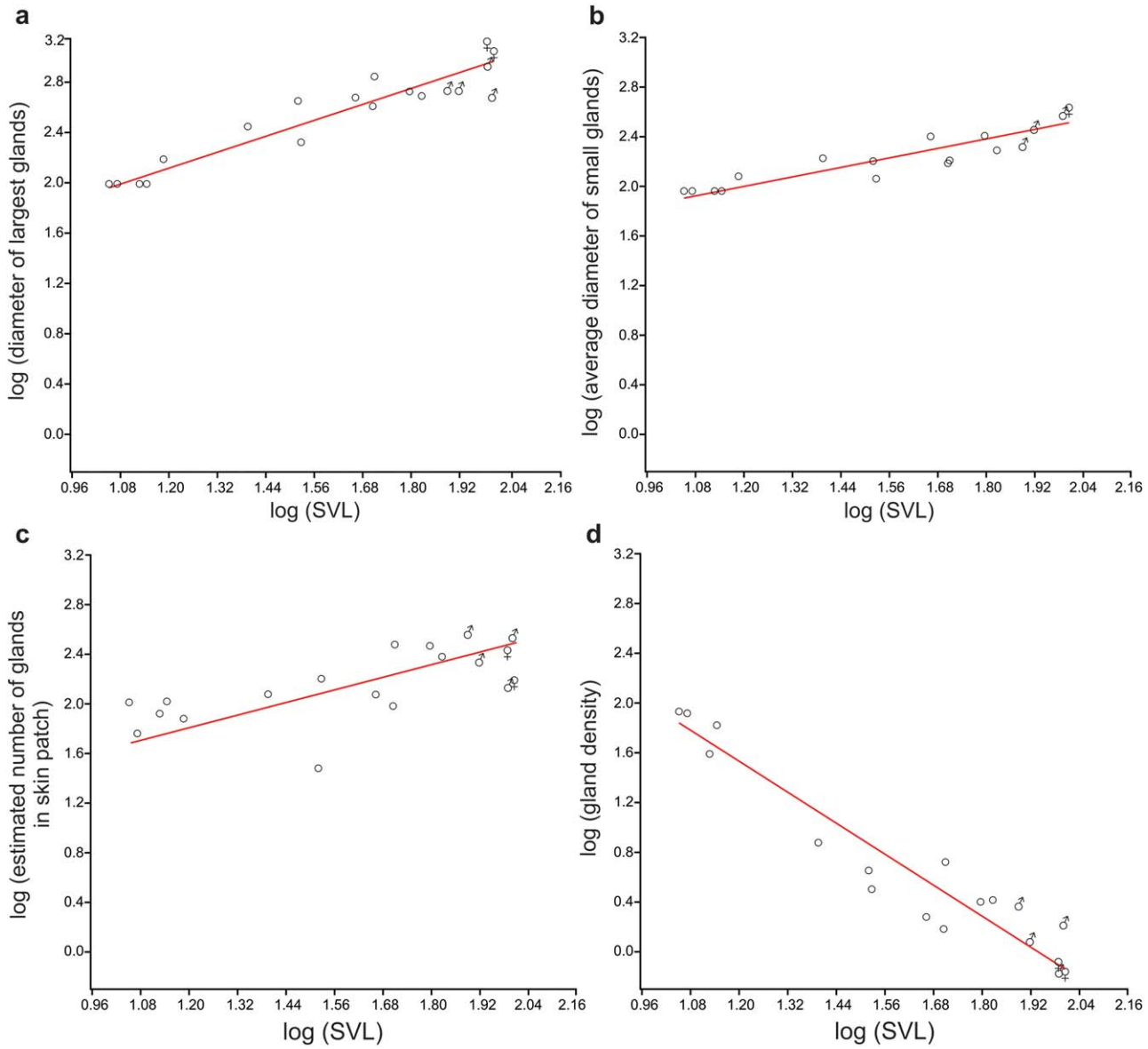

FIGURE 9 *R. arenarum*, relationship between morphometric parameters of dorsum glands and body length in *R. arenarum*. (a) diameter of largest glands ($n = 19$), (b) average diameter of smallest glands ($n = 17$), and (d) gland density ($n = 18$). Red lines in graphs represent the RMA regression estimated line. The allometry of estimated number of glands in skin patch (c) was not studied because the coefficient of determination (R^2) of the lineal regression was below the criteria established as acceptable fitness ($n = 19$). Juveniles are indicated by circles, and males and females are indicated by their respective symbols. Outliers were eliminated when necessary to fit with statistical assumptions

R. arenarum, Chammas et al. (2015) observed in *Rhinella granulosa* that the frequency of granular glands (number of skin glands/10 mm of skin) decreases with body size. Strikingly, frequency of mucous glands increases with body size, but epidermal *anlagen* of mucous glands during juvenile growth are not described. It is crucial to find out whether skin glands originate *de novo* from epidermis of post-metamorphic individuals.

Dimorphic granular glands have been described in dorsal skin of several anuran species including, *R. granulosa* (Delfino et al., 1999), *R. arenarum* (Regueira et al., 2016), *Melanophryniscus stelzneri* (Delfino, Brizzi, Kracke-Berndorff et al., 1998), and *Phyllomedusa hypochondrialis* (Delfino, Brizzi, Alvarez, et al., 1998). Particularly in *R. arenarum*, Type B granular glands seem to be restricted to the largest warts, and were not observed in juveniles or in the dorsal skin patch covering pre-sacral vertebrae. *R. arenarum* not only has different types of granular glands regarding the type of secretion but also Type A glands can be divided into small and large granular glands. Interestingly, these glands have a different growth rate during development, which increases the difference between the sizes of both glands. While small glands grew at a minor rate than body size, large glands grew at the same rate, resulting in smaller small glands along ontogeny. By the end of metamorphosis, all granular glands look the same (Regueira et al., 2016), but then, only some glands become the largest Type A glands. It would be interesting to study whether all glands are potentially large glands, and if different environmental circumstances, internal or external, trigger differences in the growth rate. For example, Licht (1967) observed that in three

species of Bufonidae, larger individuals appear to develop the parotoid gland faster, suggesting that size of an individual might modify gland development. In *R. arenarum*, large glands of the parotoid region are found by the end of metamorphosis (Regueira et al., 2016), but these glands differentiate into large peripheral and central glands only when SVL exeeds 33.09 mm. Such a delayed skin gland differentiation has not been reported previously.

The external morphology of parotoid glands is species specific (Almeida et al., 2007; Gallardo, 1987; Jared et al., 2009; Jared et al., 2014; Mailho-Fontana et al., 2014), and a particular feature of *R. arenarum* is that the macrogland has a triangle-shaped ventral extension with large peripheral glands. The function of the protein-rich gland secretion present in peripheral glands is unknown; however, the presence of large glands with an intermediate appearance between central and peripheral glands (see Figure 4a) suggests that peripheral glands could be an initial stage of maturation of central glands. Similarly, parotoids of *Anaxyrus regularis* possess granular glands at various stages of development (Toledo & Jared, 1995). At the beginning of the secretory cycle, granules have a protein material, but at more advanced stages, granules contain serotonin, a type of catecholamine. Finally, mature glands display lipid content in the secretion (Toledo & Jared, 1995). In *R. arenarum*, peripheral glands were always positive for proteins and negative for catecholamines; however, it cannot be rule out their potential capacity to produce catecholamines and a lipid-derived secretion.

A particular characteristic of parotoids in *R. arenarum*, is the presence of intraepithelial glands in the duct of the large glands. To our knowledge, this is the first report of the presence of syncytial glands with mucous secretion in the epithelium of a gland duct, and the function of this secretion is unknown.

ACKNOWLEDGMENTS

Research support was provided by UBACyT 2014–2017 no. 20020130100828BA of the Universidad de Buenos Aires, República Argentina. Scholarship support for E.R. and M.E.A.O. was provided by the Consejo Nacional de Investigaciones Científicas y Técnicas (CONICET). We thank Raul O. Gómez for his invaluable assistance in collecting specimens, using the PAST software and discussing many aspects of the study. Raúl O. Gómez and Ariel López provided pictures of *R. arenarum* in the field. Marissa Fabrezi made valuable suggestions on planning this study and the manuscript.

REFERENCES

Almeida, D. P., Felsemburgh, F. A., Azevedo, R. A., & Brito-Gitirana, D. L. (2007). Morphological re-evaluation of the parotoid glands of *Bufo ictericus* (Amphibia, Anura, Bufonidae). *Contributions to Zoology*, *76*, 145–152.

Antoniazzi, M. M., Neves, P. R., Mailho-Fontana, P. L., Rodrigues, M. T., & Jared, C. (2013). Morphology of the parotoid macroglands in *Phyllomedusa* leaf frogs. *Journal of Zoology*, *291*, 42–50.

Azevedo, R. A., Pelli, A. A., Ferreira-Pereira, A., de Jesus Santana, A. S., Felsemburgh, F., & de Brito-Gitirana, L. (2005). Structural aspects of the Eberth-Katschenko layer of *Bufo ictericus* integument: Histochemical characterization and biochemical analysis of the cutaneous calcium (Amphibian, Bufonidae). *Micron*, *36*, 61–65.

Brunetti, A. E., Hermida, G. N., & Faivovich, J. (2012). New insights into sexually dimorphic skin glands of anurans: The structure and ultrastructure of the mental and lateral glands in *Hypsiboas punctatus* (Amphibia: Anura: Hylidae). *Journal of Morphology*, *273*, 1257–1271.

Brunetti, A. E., Hermida, G. N., Luna, M. C., Barsotti, A. M., Jared, C., Antoniazzi, M. M., Rivera-Correa, M., Berneck, B. V. M., & Faivovich, J. (2015). Diversity and evolution of sexually dimorphic mental and lateral glands in Cophomantini treefrogs (Anura: Hylidae: Hylinae). *Biological Journal of the Linnean Society*, *114*, 12–34.

Chammas, S. M., Carneiro, S. M., Ferro, R. S., Antoniazzi, M. M., & Jared, C. (2015). Development of integument and cutaneous glands in larval, juvenile and adult toads (*Rhinella granulosa*): A morphological and morphometric study. *Acta Zoologica*, *96*, 460–477.

Clarke, B. T. (1997). The natural history of amphibian skin secretions, their normal functioning and potential medical applications. *Biological Reviews of the Cambridge Philosophical Society*, *72*, 365–379.

Cunha Filho, G. A., Schwartz, C. A., Resck, I. S., Murta, M. M., Lemos, S. S., Castro, M. S., Kyaw, C., Pires Jr., O. R., Leite, J. R. S., Bloch Jr, C., & Schwartz, E. F. (2005). Antimicrobial activity of the bufadienolides marinobufagin and telocinobufagin isolated as major components from skin secretion of the toad *Bufo rubescens*. *Toxicon*, *45*, 777–782.

Daly, J. W. (1995). The chemistry of poisons in amphibian skin. *Proceedings of the National Academy of Sciences of the United States of America*, *92*, 9–13.

Daly, J. W., Spande, T. F., & Garraffo, H. M. (2005). Alkaloids from amphibian skin: A tabulation of over eight-hundred compounds. *Journal of Natural Products*, *68*, 1556–1575.

Delfino, G., Brizzi, R., Alvarez, B. B., & Kracke-Berndorff, R. (1998). Serous cutaneous glands in *Phyllomedusa hypochondrialis* (Anura, Hylidae): Secretory patterns during ontogenesis. *Tissue Cell*, *30*, 30–40.

Delfino, G., Brizzi, R., Alvarez, B. B., & Taddei, L. (1999). Secretory polymorphism and serous cutaneous gland heterogeneity in *Bufo granulosus* (Amphibia, Anura). *Toxicon*, *37*, 1281–1296.

Delfino, G., Brizzi, R., Kracke-Berndorff, R., & Alvarez, B. (1998). Serous gland dimorphism in the skin of *Melanophryniscus stelzneri* (Anura: Bufonidae). *Journal of Morphology*, *237*, 19–32.

Duellman, W. E., & Trueb, L. (1994). *Biology of amphibians* (2nd ed.). Baltimore, MD: Johns Hopkins University Press.

Echeverría, D. D., & Filipello, A. M. (1990). Edad y crecimiento en *Bufo arenarum* (Anura: Bufonidae). *Cuadernos de Herpetología*, *5*, 25–31.

Ferraro, D. P., Topa, P. E., & Hermida, G. N. (2013). Lumbar glands in the frog genera *Pleurodema* and *Somuncuria* (Anura: Leiuperidae): Histological and histochemical perspectives. *Acta Zoologica*, *94*, 44–57.

Freeland, W. J., & Kerin, S. H. (1991). Ontogenetic alteration of activity and habitat selection by *Bufo marinus*. *Wildlife Research*, *18*, 431–443.

Gallardo, J. M. (1987). *Anfibios Argentinos: Guía para su identificación*. Buenos Aires: Librería Agropecuaria.

Hammer, Ø., Harper, D. A. T., & Ryan, P. D. (2001). PAST: Paleontological statistics software package for education and data analysis. *Palaeontol Electron*, *4*, 9.

Hayes, R. A., Crossland, M. R., Hagman, M., Capon, R. J., & Shine, R. (2009). Ontogenetic variation in the chemical defenses of cane toads (*Bufo marinus*): Toxin profiles and effects on predators. *Journal of Chemical Ecology*, *35*, 391–399.

IUCN. (2016). The IUCN Red List of Threatened Species. Version 2016-2. Retrieved from http://www.iucnredlist.org (accessed on 04 September, 2016).

Jared, C., Antoniazzi, M. M., Jordão, A. E. C., Silva, J. R. M. C., Greven, H., & Rodrigues, M. T. (2009). Parotoid macroglands in toad (*Rhinella jimi*): Their structure and functioning in passive defence. *Toxicon*, *54*, 197–207.

Jared, C., Antoniazzi, M. M., Navas, C. A., Katchburian, E., Freymüller, E., Tambourgi, D. V., & Rodrigues, M. T. (2005). Head co-ossification, phragmosis and defence in the casque-headed tree frog *Corythomantis greeningi*. *Journal of Zoology*, *265*, 1–8.

Jared, S. G., Jared, C., Egami, M. I., Mailho-Fontana, P. L., Rodrigues, M. T., & Antoniazzi, M. M. (2014). Functional assessment of toad parotoid macroglands: A study based on poison replacement after mechanical compression. *Toxicon*, *87*, 92–103.

Jeckel, A. M., Saporito, R. A., & Grant, T. (2015). The relationship between poison frog chemical defenses and age, body size, and sex. *Frontiers in Zoology*, *12*, 1.

Kiernan, J. (1999). *Histological and histochemical methods: Theory and practice* (3rd ed.). Oxford, UK: Butterworth Heinemann.

Lenzi-Mattos, R., Antoniazzi, M. M., Haddad, C. F. B., Tambourgi, D. V., Rodrigues, M. T., & Jared, C. (2005). The inguinal macroglands of the frog *Physalaemus nattereri* (Leptodactylidae): Structure, toxic secretion and relationship with deimatic behaviour. *Journal of Zoology*, *266*, 385–394.

Licht, L. E. (1967). Initial appearance of the parotoid gland in three species of toads (genus *Bufo*). *Herpetologica*, *23*, 115–118.

Maciel, N. M., Collevatti, R. G., Colli, G. R., & Schwartz, E. F. (2010). Late Miocene diversification and phylogenetic relationships of the huge toads in the *Rhinella marina* (Linnaeus, 1758) species group (Anura: Bufonidae). *Molecular Phylogenetics and Evolution*, *57*, 787–797.

Maciel, N. M., Schwartz, C. A., Pires, O. R., Sebben, A., Castro, M. S., Sousa, M. V., Fontes, W. & Schwartz, E. N. F. (2003). Composition of indolealkylamines of *Bufo rubescens* cutaneous secretions compared to six other Brazilian bufonids with phylogenetic implications. *Comparative Biochemistry and Physiology—Part B*, *134*, 641–649.

Mailho-Fontana, P. L., Antoniazzi, M. M., Toledo, L. F., Verdade, V. K., Sciani, J. M., Barbaro, K. C., Pimenta, D.C., Rodrigues, M. T., & Jared, C. (2014). Passive and active defense in toads: The Parotoid Macroglands in *Rhinella marina* and *Rhaebo guttatus*. *Journal of Experimental Zoology Part A*, *321*, 65–77.

Navas, C. A., Jared, C., & Antoniazzi, M. M. (2002). Water economy in the casque-headed tree-frog *Corythomantis greeningi* (Hylidae): Role of behaviour, skin, and skull skin co-ossification. *Journal of Zoology*, *257*, 525–532.

Phillips, B. L., & Shine, R. (2006). Allometry and selection in a novel predator prey system: Australian snakes and the invading cane toad. *Oikos*, *112*, 122–130.

Portik, D. M., & Papenfuss, T. J. (2015). Historical biogeography resolves the origins of endemic Arabian toad lineages (Anura: Bufonidae): Evidence for ancient vicariance and dispersal events with the Horn of Africa and South Asia. *BMC Evolutionary Biology*, *15*, 1.

Quinzio, S., & Fabrezi, M. (2012). Ontogenetic and structural variation of mineralizations and ossifications in the integument within ceratophryid frogs (Anura, Ceratophryidae). *The Anatomical Record*, *295*, 2089–2103.

Rash, L. D., Morales, R. A., Vink, S., & Alewood, P. F. (2011). De novo sequencing of peptides from the Parotoid secretion of the cane toad, *Bufo marinus* (*Rhinella marina*). *Toxicon*, *57*, 208–216.

Regueira, E., Dávila, C., & Hermida, G. N. (2016). Morphological changes in skin glands during development in *Rhinella arenarum* (Anura: Bufonidae). *The Anatomical Record*, *299*, 141–156.

Saporito, R. A., Isola, M., Maccachero, V. C., Condon, K., & Donnelly, M. A. (2010). Ontogenetic scaling of poison glands in a dendrobatid poison frog. *Journal of Zoology*, *282*, 238–245.

Schmidt-Nielsen, K. (1984). *Scaling: Why is animal size so important*? Cambridge, UK: Cambridge University Press.

Sciani, J. M., Angeli, C. B., Antoniazzi, M. M., Jared, C., & Pimenta, D. C. (2013). Differences and similarities among parotoid macrogland secretions in South American toads: A preliminary biochemical delineation. *The Scientific World Journal*, *2013*, 1–9.

Terreni, A., Nosi, D., Greven, H., & Delfino, G. (2003). Development of serous cutaneous glands in *Scinax nasica* (Anura, Hylidae): Patterns of poison biosynthesis and maturation in comparison with larval glands in specimens of other families. *Tissue Cell*, *35*, 274–287.

Toledo, R. C., & Jared, C. (1993). Cutaneous adaptations to water balance in amphibians. *Comparative Biochemistry and Physiology—Part A*, *105*, 593–608.

Toledo, R. C., & Jared, C. (1995). Cutaneous granular glands and amphibian venoms. *Comparative Biochemistry and Physiology—Part A*, *111*, 1–29.

Toledo, R. C., Jared, C., Brunner, A. B., Jr. (1992). Morphology of the large granular alveoli of the parotoid glands in toad (*Bufo ictericus*) before and after compression. *Toxicon*, *30*, 745–753.

Vaira, M., Akmentins, M. S., Attademo, M., Baldo, D., Barrasso, D., Barrionuevo, S., Basso, N., Blotto, B., Cairo, S., Cajade, R., Céspedes, J., Corbalán, V., Chilote, P., Duré, M., Falcione, C., Ferraro, D., Gutierrez, F. R., Ingaramo, M. R., Junges, C., Lajmanovich, R., Lescano, J. N., Marangoni, F., Martinazzo, L., Marti, R., Moreno, L., Natale, G. S., Perez Iglesias, J. M., Peltzer, P., Quiroga, L., Rosset, S., Sanabria, E., Sanchez, L., Schaefer, E., Úbeda, C., & Zaracho, V. (2012). Categorización del estado de conservación de los anfibios de la República Argentina. *Cuadernos de Herpetología*, *26*, 131–159.

Vences, M., Wahl-Boos, G., Hoegg, S., Glaw, F., Spinelli Oliveira, E., Meyer, A., & Perry, S. (2007). Molecular systematics of mantelline frogs from Madagascar and the evolution of their femoral glands. *Biological Journal of the Linnean Society*, *92*, 529–539.

Warton, D. I., Wright, I. J., Falster, D. S., & Westoby, M. (2006). Bivariate line-fitting methods for allometry. *Biological Reviews*, *81*, 259–291.

How to cite this article: Regueira E, Dávila C, Sassone AG, O'Donohoe MEA, Hermida GN. Post-metamorphic development of skin glands in a true toad: Parotoids versus dorsal skin. *Journal of Morphology*. 2017;00:1–13. https://doi.org/10.1002/jmor.20661.